Key Engineering Materials
ISSN: 1662-9795, Vol. 926, pp 168-175
doi:10.4028/p-g9is26

Submitted: 2021-12-08
Accepted: 2022-01-24
Online: 2022-07-22

Acoustic Performances of Polymers Hierarchical Structure Produced with Material Jetting Technology

Levi E.[1,a], Piana E.[1,b*], Giorleo L.[1,c]

[1]Department of Mechanical and Industrial Engineering, University of Brescia, Italy

[a]elisa.levi@unibs.it; [b]edoardo.piana@unibs.it, [c]luca.giorleo@unibs.it

Keywords: Hierarchical structure, Additive Manufacturing, Acoustic properties of materials

Abstract. This research is aimed at testing the ability of high-end 3D printers to reproduce complex structures having some acoustic performances in terms of sound absorption and sound transmission loss. Specifically, some experiments were made on four different types of geometries to compare their acoustic behaviour. The sound absorption and sound insulation of the samples have been evaluated by means of a four-microphone impedance tube. The adopted technique allows to retrieve the transfer matrix of each specimen and then, through a composition of the matrices, to virtually determine the acoustic performances of any arrangement of the different samples. The experiments revealed promising results in terms of quality, finishing and precision of the jetting process, highlighting benefits and critical issues related to the acoustic performances.

Introduction

Nowadays, a revolution in workpiece geometries design is taking place thanks to the ability of Additive Manufacturing (AM) to produce complex shapes avoiding all the constraints typical of conventional manufacturing processes. These characteristics can be exploited in the design of new solutions that can be applied to different fields from aeronautical to biomedical [1, 2]. In this work, particular attention has been paid on the ability of additive manufacturing to produce hierarchical structures possessing acoustic properties. These structures are commonly referred as non-stochastic cellular material and are governed by mathematical relationships [3]. The hierarchical structures, coupled with the concept of topology optimization, proved to be effective methods to reduce the weight of mechanical parts. However, in the last decade new application fields started to be under investigation. Among these, acoustic performances could gain benefits from the complexity of hierarchical structures to control properties like reflection/absorption, insulation, band filtering, and scattering [4, 5]. In literature a few studies can be found on this topic, in particular different lattice structures produced with fused filament fabrication [6-8]. Most of the research put into evidence how AM easily allows to produce structures able to absorb or reflect a range of frequencies as a function of cell design. Despite these benefits, it must be reported that the most used hierarchical structure is a combination of two layers: a first one with parallel rods and a second one with same parallel rods placed orthogonal to the first structure. In this way the porosity, defined as the hatching distance imposed to two consecutive rods of the specimen, can be controlled.

To enhance the knowledge about this topic, in this article the acoustic properties of four different kinds of lattice structures which are commonly used in part design have been measured and compared. The results highlighted that the acoustic performances of such structures are exploitable in a limited frequency range. Nonetheless, by wisely combining the single geometries it is possible to build a structure featuring extended acoustic properties.

Materials and Methods

In this research four base cases have been selected for a first characterisation. Such base cases can be defined by the different single cell geometry: sphere with truncated ends (Fig. 1a), Diamond (Fig. 1b), Schwartz-D (Fig. 1c) and Gyroid (Fig. 1d). The first geometry is already used in the acoustic field since it can be easily associated to a given porosity, while the other ones find application in the mechanical field, when there is the need to reduce the weight of some parts without significantly

modifying the mechanical performances. Fig. 1 shows the single cell geometry and the main dimensions.

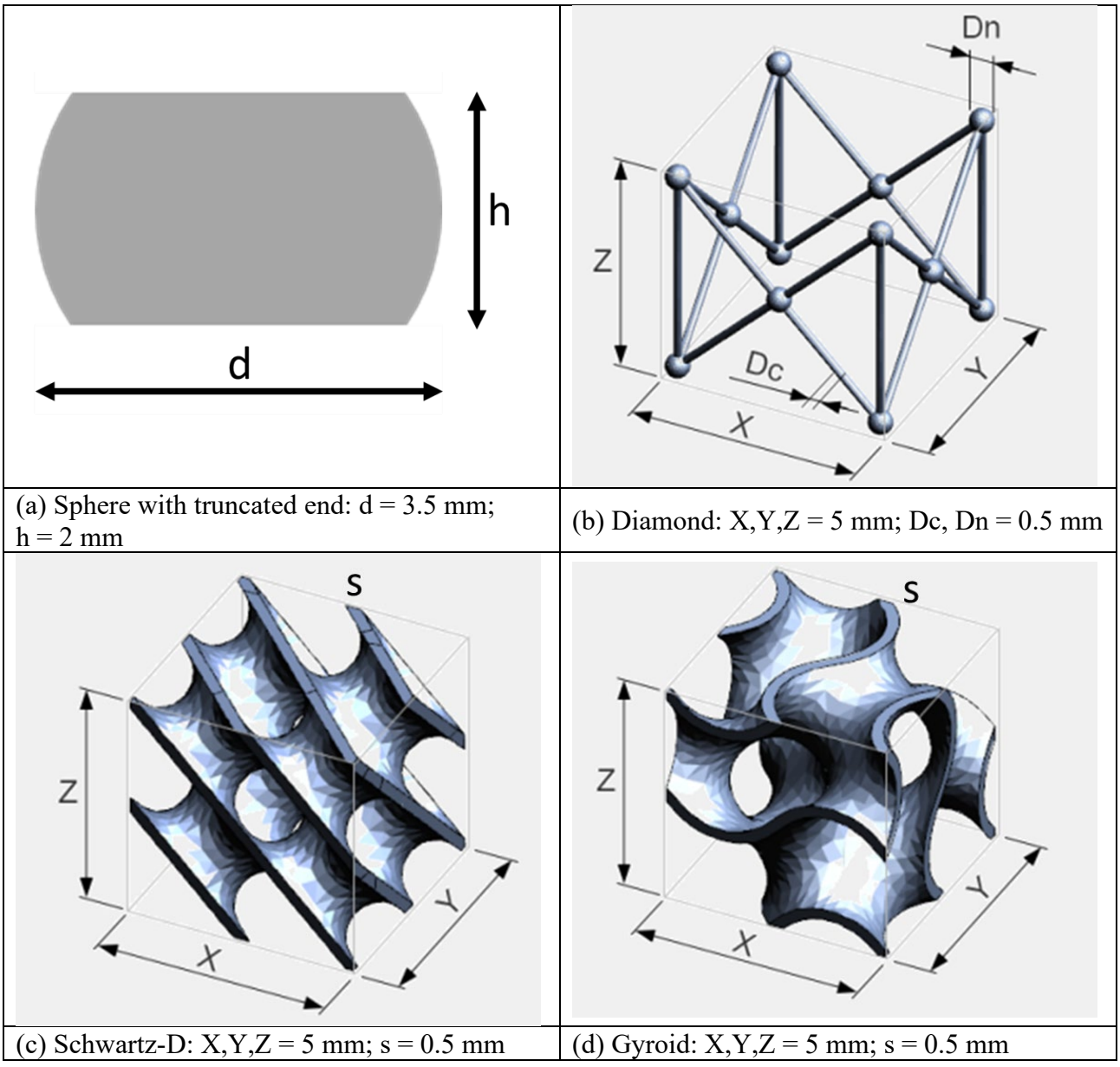

(a) Sphere with truncated end: d = 3.5 mm; h = 2 mm

(b) Diamond: X,Y,Z = 5 mm; Dc, Dn = 0.5 mm

(c) Schwartz-D: X,Y,Z = 5 mm; s = 0.5 mm

(d) Gyroid: X,Y,Z = 5 mm; s = 0.5 mm

Figure 1: Single cell geometry description.

Once the single cell geometry is defined, the specimens have been designed imposing a linear cell array for the Sphere, Swartz-D and Gyroid geometries. A radial array has been used for the Diamond case. To perform the acoustic tests, the specimens must be placed inside a holder. Such holder is a hollow cylinder having an internal diameter of 46 mm. The thickness of the specimens has been selected so to be coherent with the dimension of the single cells for all the chosen geometries. To avoid gaps between the specimens and the sample holder, a 3 mm thick annulus has been left at the external side of the array. A triangular cross section shape was added on the top of the 3 mm thick annulus. On the opposite side, at the bottom part of the annulus, cavities where the triangular shapes can be used as centring snaps have been obtained, so to have a reference for the positioning of different samples assembled in a stack.

The specimens were produced with a Project 2500 Pro machine (3D System, South Caroline, US) that works with Material Jetting technology; this technology is an inkjet printing process using piezo printhead technology to deposit photocurable plastic resin droplets layer by layer. This Additive Manufacturing technology ensures precise production (single layer thickness 25 μm) and high part

complexity design because it uses wax as support material. Three specimens have been produced for each case study (overall thickness of the samples 20 mm). Fig. 2 displays the drawings of each type of sample produced.

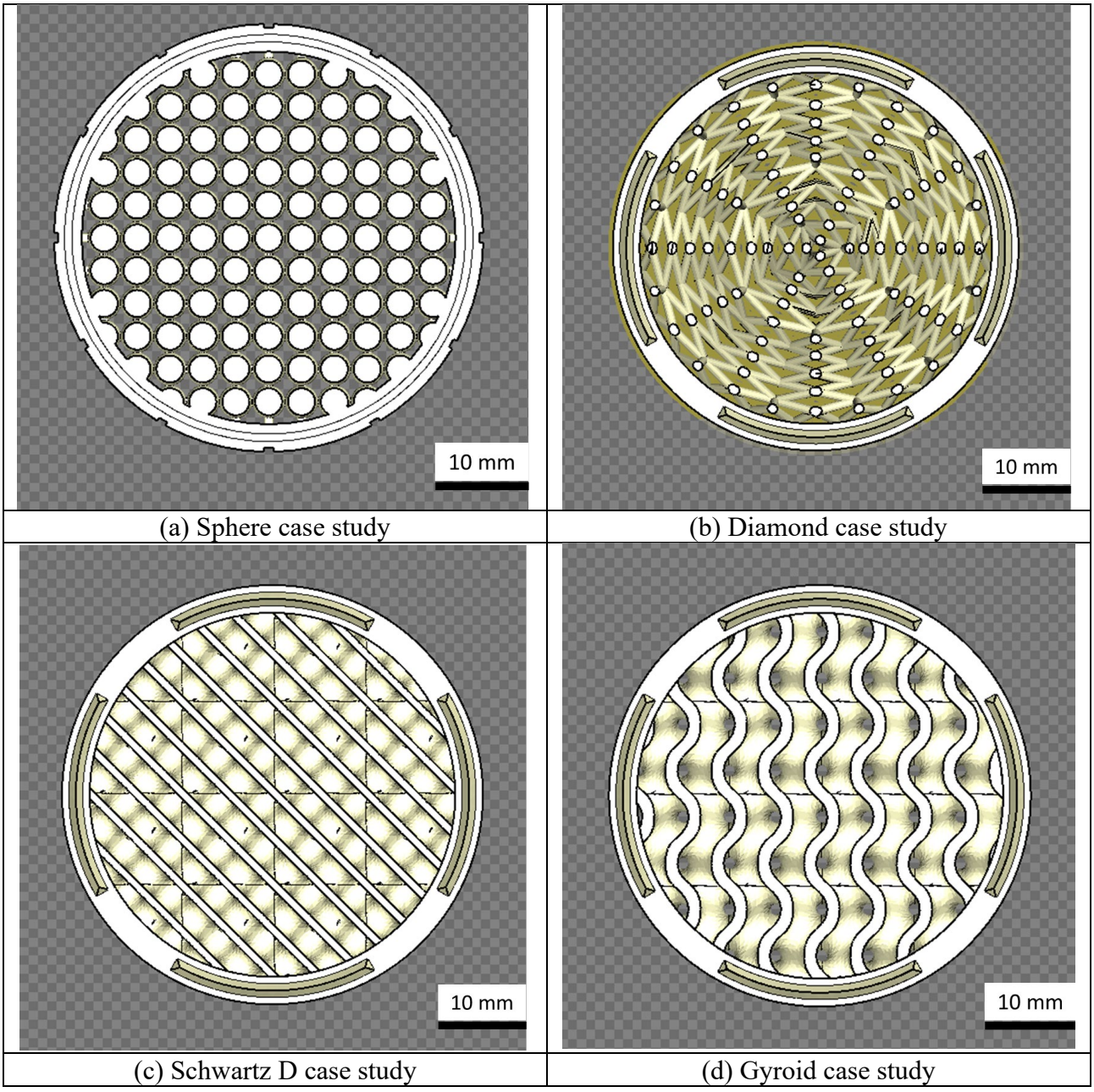

(a) Sphere case study (b) Diamond case study

(c) Schwartz D case study (d) Gyroid case study

Figure 2: Geometries considered as case studies.

The acoustic performances of the four specimens were measured by means of a four-microphone impedance tube using the transfer matrix approach, following the procedure provided by the ASTM E2611 standard [9]. This method allows to easily obtain the estimation of the sound absorption coefficient α, which expresses the dissipation of the sound energy inside the tested specimen, and of the sound transmission loss *TL*, which describes the sound insulation capability.

As shown by the schematic drawing of Fig. 3, the four-microphone impedance tube is composed by a double standing wave tube. Each section is equipped with a microphone pair. One endpoint of the tube features a loudspeaker, properly isolated and sealed, which is connected to a multichannel analyser. The test signal used during the experiments was a pink noise in the frequency band 20 Hz – 5 kHz. The other end can be limited by either anechoic or reflective termination. The central section of the tube is the sample holder. This is a detachable unit made of a suitable long segment of tube

where the specimen is placed. One microphone pair is mounted in front of the sample, the other pair close to the back side of the sample. This configuration allows to compare the signals from the four microphones so to decompose the resulting upstream and downstream sound field into forward (A and C) and backward (B and D) travelling waves.

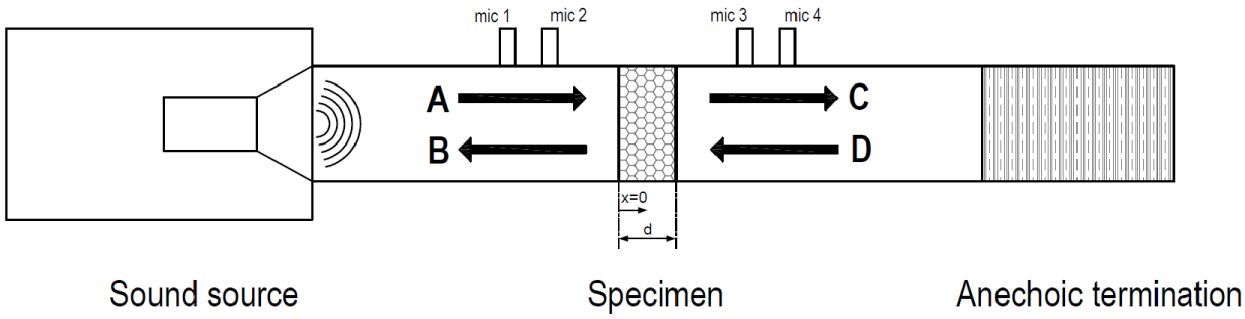

Figure 3: Schematic drawing of a four-microphone impedance tube.

The transfer matrix approach, applied to the four-microphone impedance tube, allows to build the relationship between the state variables at the two sides of the sample. Specifically, these quantities are the particle velocities (u_i) and the sound pressures (p_i) on the front ($x=0$) and back ($x=d$) surfaces of the sample. The resulting relationship, including the transfer matrix $\boldsymbol{T}$, can be written as:

$$\begin{bmatrix} p_0 \\ u_0 \end{bmatrix} = \begin{bmatrix} T_{11} & T_{12} \\ T_{21} & T_{22} \end{bmatrix} \begin{bmatrix} p_d \\ u_d \end{bmatrix} = \boldsymbol{T} \begin{bmatrix} p_d \\ u_d \end{bmatrix} \tag{1}$$

The above-mentioned wave components A, B, C, D (incident and reflected fractions) can be used to compute the transfer matrix elements T_{ij} by following the expressions provided by ASTM E2611 standard. Finally, the acoustic properties of the sample can be calculated as a function of the transfer matrix elements; in particular, the absorption coefficient α can be expressed as:

$$\alpha = 1 - \left| \frac{T_{11} - \rho c T_{21}}{T_{11} + \rho c T_{21}} \right|^2 \tag{2}$$

while the sound transmission loss TL is obtained as:

$$TL = 20 \log \left| \frac{T_{11} + (T_{12}/\rho c) + T_{21} \rho c + T_{22}}{2 \times exp\,(jkd)} \right| \tag{3}$$

where c is the speed of sound, ρ is the air density and k is the wavenumber in air, defined as $k = 2\pi f / c$.

The Applied Acoustics Laboratory at the University of Brescia is equipped with a custom-made impedance tube (Fig. 4), composed of two 1200 mm long standing wave tubes with an inner diameter of 46 mm. Such dimension allows to satisfy the plane-wave assumption up to about 3700 Hz. The microphone ports are located 45 mm apart one from the other. Using such configuration, the useful frequency range for the determination of the acoustic properties of the specimens goes from 100 Hz to 3500 Hz.

An OROS OR36 multichannel analyser is connected to the loudspeaker, so to generate the plane wave field inside the tube. The same analyser is able to acquire and post process the signals coming from the transducers (four ¼" PCB 130F22 microphones), thus measuring the complex transfer functions between the microphone positions. The microphones are calibrated using a Bruel and Kjaer 4228 pistonphone before the tests. To guarantee the air tightness, the various elements composing the entire measurement system are sealed with O-rings.

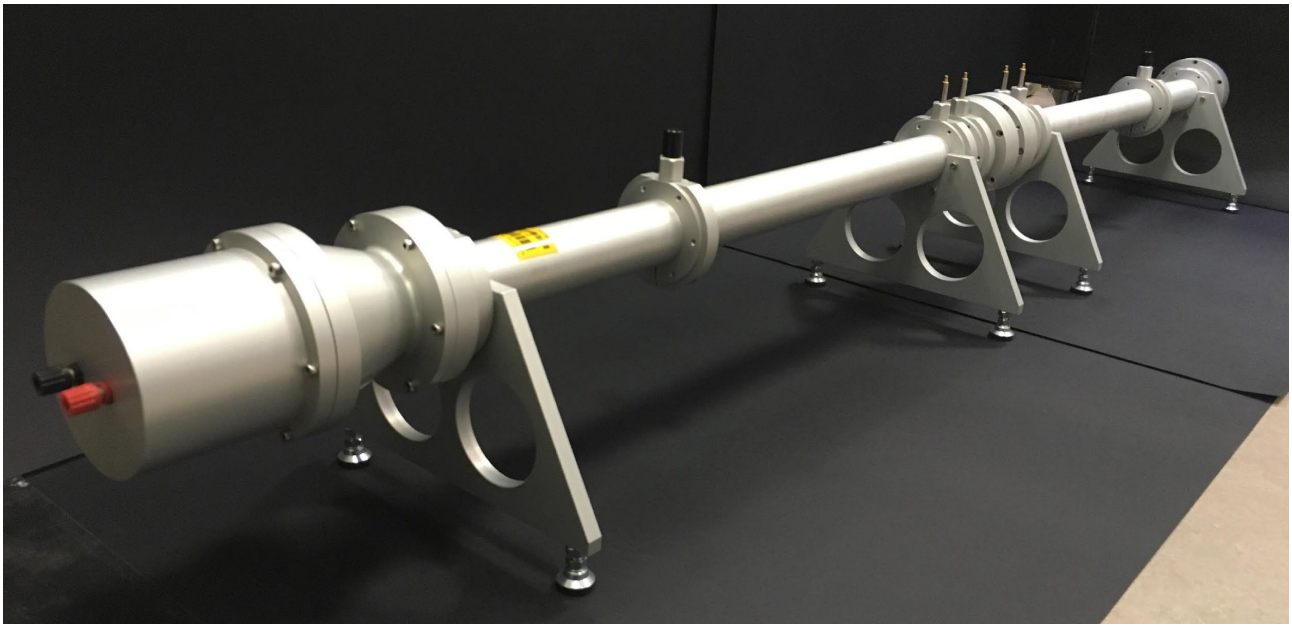

Figure 4: Image of the four-microphone impedance tube.

The post-processing of the measured transfer functions was performed by means of a MATLAB script that allows to determine the acoustic parameters of the specimen.
The main advantages of this measurement technique are that it requires the use of small samples, the set-up and measurement phases are fast, and in addition to α and TL it also provides further useful properties, such as the speed of sound inside the sample, the characteristic impedance, and the propagation wavenumber. Nevertheless, it can be used to estimate the sound absorption and the sound transmission loss only in the case of normal sound incidence.
The transfer matrix approach is proved to be a particularly convenient method when dealing with the acoustic characterisation and optimisation of multi-layered structures: the acoustic properties of a specimen composed by different layers can be derived from the total transfer matrix, which results from the product of the individual transfer matrices of each layer:

$$\boldsymbol{T_{total} = T_1 \cdot T_2 \cdot \ldots \cdot T_N} \tag{4}$$

Results

This section shows the experimental results for the sound absorption coefficient and for the sound transmission loss of the four specimens. Fig. 5 collects the sound absorption results.

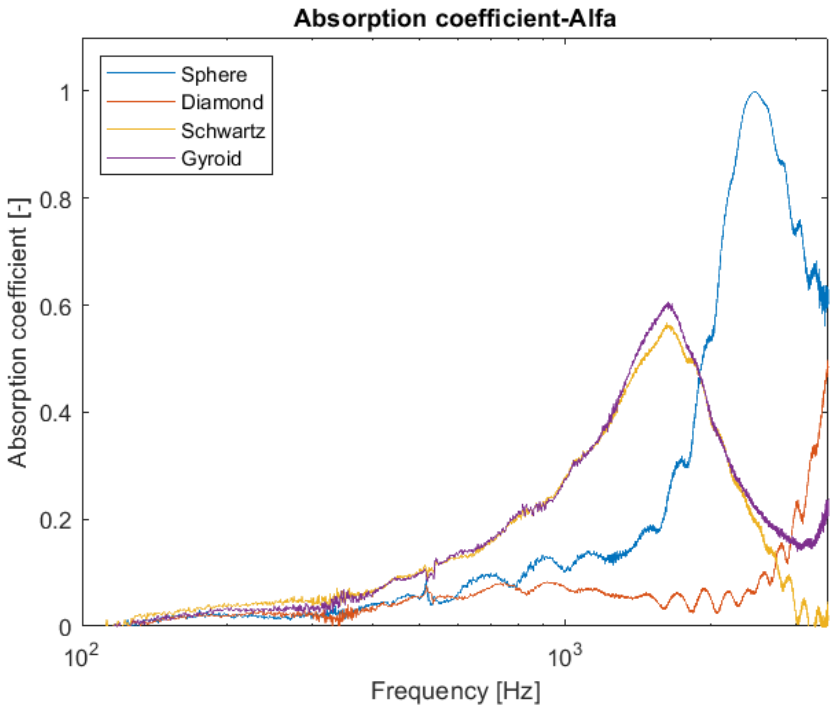

Figure 5: Normal incidence sound absorption coefficient of the four specimens.

The Sphere sample features the highest sound absorption, with the theorical maximum value of 1 around 2500 Hz. As concerns the Diamond sample, the geometry is characterised by a very low porosity. For this reason, the sound can pass through the specimen without being impeded in its propagation and the resulting sound absorption is very low up to 2500 Hz. For higher frequencies the absorption coefficient increases, with a maximum of 0.55 around 3200 Hz. The Schwartz and the Gyroid samples are based on the same basic geometry but are the negative one of the other. For this reason, their absorption behaviour is very similar, featuring a maximum value of 0.55-0.6 around 1600 Hz. In all the cases, being the samples relatively thin, the sound absorption in the low frequency range cannot reach values of interest for real life applications.

Fig. 6 shows the results of the tests as concerns the sound Transmission Loss. The comments of the results in this case must take into account the meaning of this quantity, expressing the capability of the specimen not to be crossed by sound waves. The Sphere specimen is the one with the lowest porosity but also with the highest flow resistivity. For this reason, it shows a *TL* comparable to the ones of the Diamond and Schwartz specimens up to 1000 Hz, but then the characteristic of the surface brings to a degradation of this parameter in favour of the sound absorption. Also for the transmission loss results the Diamond and the Schwartz specimens show very similar behaviours, with a *TL* plot always increasing with a slope that becomes higher than the one visible in the medium frequency range above 2000 Hz. Finally, as concerns the Diamond specimens, the *TL* is poor in the entire frequency range of interest.

Given the results reported henceforth, it can be of interest to understand if it is possible to compose the specimens considered in this study so to obtain higher sound absorption or sound *TL* values in the frequency range where the single specimens have presented poor acoustic properties. Since the specimens were physically available, a new experimental test was performed assembling the samples in the following order: Sphere (12 mm), Schwartz (20 mm), Gyroid (20 mm) and Sphere (12 mm). The outcome of the measurement in terms of sound absorption coefficient is shown in Fig. 7. It can be noted that the absorption coefficient is completely different from the ones given in Fig. 5 and the maximum value is now at 2000 Hz, with a second relative maximum of 0.78 at 680 Hz. Such result can be derived also composing the different transfer matrices once the specimens have been tested using the four-microphone impedance tube, thus avoiding further experimental tests, and allowing in advance to design the material by optimising the layers sequence as a function of the acoustic characteristics needed for a particular application.

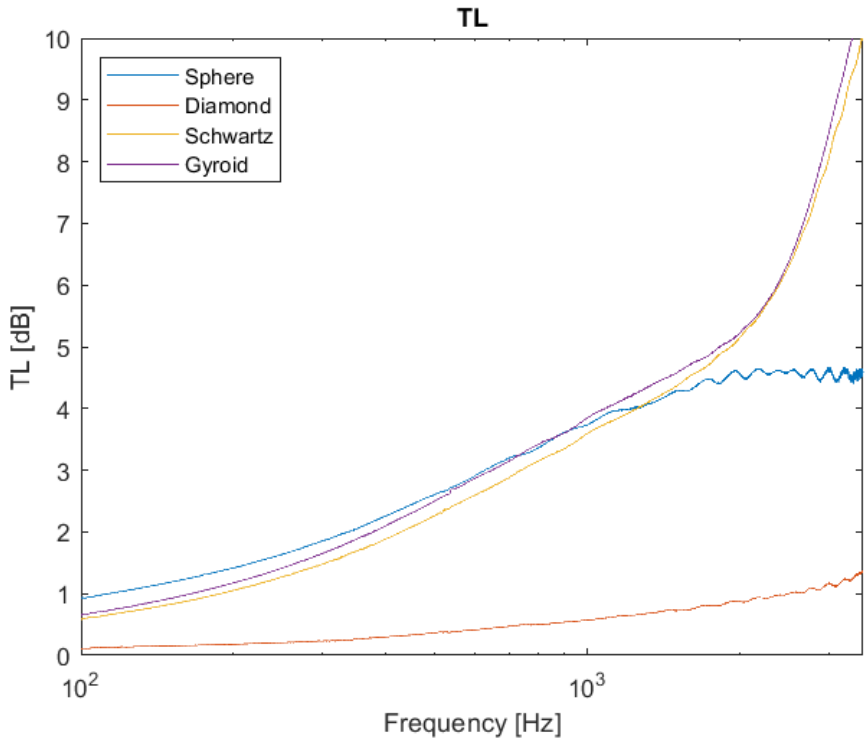

Figure 6: Sound Transmission Loss of the four specimens.

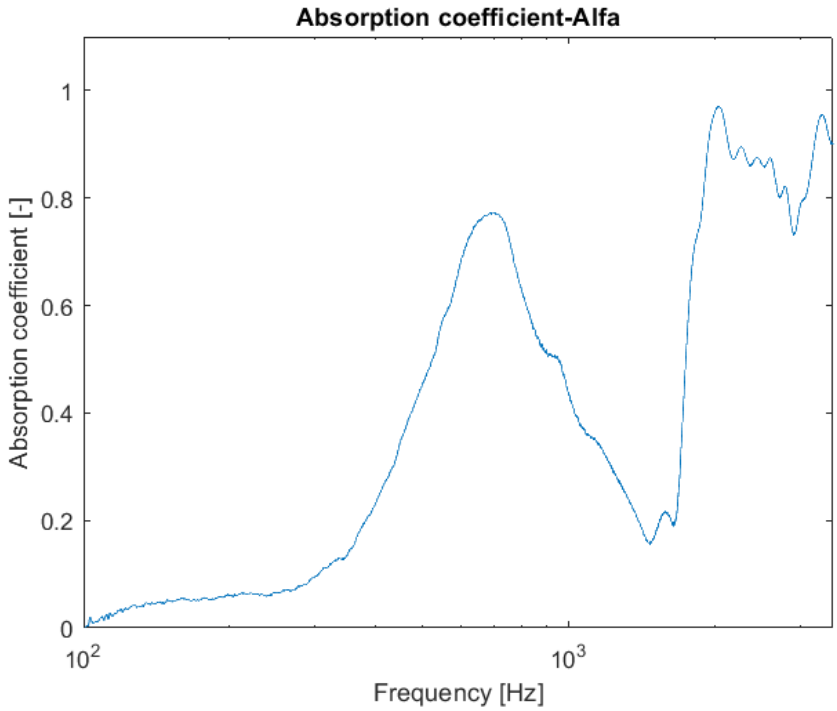

Figure 7: Sound absorption of a specimen composed by the following sequence: Sphere (12 mm), Schwartz (20 mm), Gyroid (20 mm) and Sphere (12 mm).

Conclusions

This paper investigates the acoustic performances, in terms of sound absorption and sound transmission loss, of polymers hierarchical structures produced with material jetting technology. Four base cases have been selected for the tests, with different geometries of the single cell: Sphere with truncated ends, Diamond, Schwartz-D, and Gyroid. The acoustic characterisation of the four

specimens featuring the four lattice structures was performed by means of the transfer matrix approach applied to the four-microphone impedance tube method.
The results show that each specimen has specific strengths and critical issues, the latter due to the fact that the frequency range of interest for the acoustic performances is limited.
Based on considerations related to the geometrical characteristics and porosity of the base cases, a specific combination of the specimens was then tested with the aim to improve the sound absorption in the mid frequency range. The result obtained from the experiment is promising.
In addition, it is worth to highlight that, once the transfer matrices of each base specimen are experimentally obtained, the acoustic properties of a given combination of the single geometries can be estimated without further experimental tests. The advantage of this method is to allow to optimise the layer sequence in order to improve the acoustic performance according to the specific need or application. This is the reason why the authors will further investigate this aspect in a future research, modulating the base cell dimensions, the thickness, and the sequence of each layer.

References

[1] Gao, W., Zhang, Y., Ramanujan, D., Ramani, K., Chen, Y., Williams, C.B., Wang, C.C.L., Shin, Y.C., Zhang, S., Zavattieri, P.D. The status, challenges, and future of additive manufacturing in engineering (2015) CAD Computer Aided Design, 69, pp. 65-89. DOI: 10.1016/j.cad.2015.04.001

[2] Ligon, S.C., Liska, R., Stampfl, J., Gurr, M., Mülhaupt, R. Polymers for 3D Printing and Customized Additive Manufacturing (2017) Chemical Reviews, 117 (15), pp. 10212-10290. DOI: 10.1021/acs.chemrev.7b00074

[3] Panesar, A., Abdi, M., Hickman, D., Ashcroft, I. Strategies for functionally graded lattice structures derived using topology optimisation for Additive Manufacturing (2018) Additive Manufacturing, 19, pp. 81-94. DOI: 10.1016/j.addma.2017.11.008

[4] Liu, Z., Zhan, J., Fard, M., Davy, J.L. Acoustic properties of a porous polycarbonate material produced by additive manufacturing (2016) Materials Letters, 181, pp. 296-299. DOI: 10.1016/j.matlet.2016.06.045

[5] Fotsing, E.R., Dubourg, A., Ross, A., Mardjono, J. Acoustic properties of a periodic micro-structures obtained by additive manufacturing (2019) Applied Acoustic, 148, 322-331. DOI: 10.1016/j.apacoust.2018.12.030

[6] Boulvert, J., Costa-Baptista, J., Cavalieri, T., Perna, M., Fotsing, E.R., Romero-García, V., Gabard, G., Ross, A., Mardjono, J., Groby, J.-P. Acoustic modeling of micro-lattices obtained by additive manufacturing (2020) Applied Acoustics, 164, art. no. 107244. DOI: 10.1016/j.apacoust.2020.107244

[7] Zieliński, T.G., Opiela, K.C., Pawłowski, P., Dauchez, N., Boutin, T., Kennedy, J., Trimble, D., Rice, H., Van Damme, B., Hannema, G., Wróbel, R., Kim, S., Ghaffari Mosanenzadeh, S., Fang, N.X., Yang, J., Briere de La Hosseraye, B., Hornikx, M.C.J., Salze, E., Galland, M.-A., Boonen, R., Carvalho de Sousa, A., Deckers, E., Gaborit, M., Groby, J.-P. Reproducibility of sound-absorbing periodic porous materials using additive manufacturing technologies: Round robin study (2020) Additive Manufacturing, 36, art. no. 101564. DOI: 10.1016/j.addma.2020. 101564

[8] Zhang, X., Qu, Z., Wang, H. Engineering Acoustic Metamaterials for Sound Absorption: From Uniform to Gradient Structures (2020) iScience, 23 (5), art. no. 101110. DOI: 10.1016/j.isci.2020.101110

[9] ASTM Standard E2611-19, Test Method for Normal Incidence Determination of Porous Material Acoustical Properties Based 703 on the Transfer Matrix Method, ASTM International (2019). DOI: 10.1520/E2611-19